Optimization of Switchgrass Combustion for Simultaneous Production of Energy and Pozzolan

Yu Wang[1]; Yixin Shao, M.ASCE[2]; Miodrag Darko Matovic[3]; and Joann K. Whalen[4]

Abstract: Combustion of switchgrass, a low-carbon fuel, generates energy and ash that can be recycled as a pozzolan in cement. This study aimed to optimize switchgrass combustion to achieve high-energy conversion and ash recycling value for cement. Combustion factors under investigation included temperature (350°C, 450°C, 550°C, or 650°C) and retention time (1 h or 4 h). Energy release was quantified by thermogravimetric analysis-differential scanning calorimetry, and ash pozzolanic activity was assessed with the concrete strength test. A numeric simulation model of the pozzolanic reaction, based on unbiased experimental data from $Ca(OH)_2$-ash suspensions, provided insight into how combustion conditions affected the pozzolanic properties of switchgrass ash. Consequently, combustion at 550°C for 4 h was recommended for concurrently optimizing the ash pozzolanic activity (114%) and energy output (4.21 kJ/g) from switchgrass. **DOI: 10.1061/(ASCE)MT.1943-5533.0001312.** © *2015 American Society of Civil Engineers.*

Author keywords: Cement and concrete; Pozzolanic reaction; Compressive strength; Low carbon fuel; Kinetic simulation.

Introduction

Replacing fossil fuel with low-carbon fuel (LCF) is an emerging trend in energy-intensive industries, such as cement production, to lessen CO_2 emissions (Schneider et al. 2011). Since cement is produced via calcination in a kiln at 1,450°C, a medium-size cement plant would deplete 3–6 MJ of fossil fuel and emit 0.8 kg of CO_2 per 1 kg of cement fabricated (Huntzinger and Eatmon 2009). An energy crop like switchgrass (*Panicum vigratum L.*) is a suitable LCF because it is carbon neutral in its life cycle. Its energy value (17.5 MJ of higher heating value) is similar to other cost-effective biomass already used as industrial LCF (17–21 MJ/kg) (Yin 2011). A LCF energy generation unit can be set along with the cement calcination process to produce green energy (Fig. 1). Compared to cofiring inside the kiln, this strategy lowers the capital cost and technical difficulty of using LCF energy for cement production and also has a high flexibility for LCF energy unit configuration. Consequently, this concept can make the cement plant reduce its fossil fuel consumption and carbon footprint accordingly.

Biomass energy is normally generated via combustion at temperatures between 300 and 700°C in a normal air atmosphere, which can be achieved efficiently in an independent biomass combustor (e.g., moving-grate boiler or fluidized bed) that produces heat, steam, or electricity (Jenkins et al. 1998). Substituting 5% or 20% (by calorific value) of fossil energy with switchgrass energy (4.62% ash content and 17.5 MJ/kg of energy value) would produce 1.39 kg or 5.54 kg of ash generated on site per 1,000 kg of cement produced (Wang et al. 2014b). This ash is usually an industrial solid waste owing to its fine particle size (≤ 5 μm) and mineral-rich properties (e.g., Si, Fe, Na, K, Ca $\geq$ 85% by weight) (Monti et al. 2008). Any cement plant that considers using switchgrass as LCF must develop an ash disposal plan that is economical and sustainable.

Since the switchgrass combustion unit (e.g., moving-grate boiler) is independent from cement calcination, it is possible to collect and dispose of switchgrass ash by substituting a part of cement with the ash for concrete making (Fig. 1). If ash possesses satisfactory physiochemical properties (e.g., rich in $SiO_2+Al_2O_3+Fe_2O_3$ but low content of carbon and alkali metals, and with an evidently amorphous structure), it can be considered as an additive with similar functions as silica fume, metakaolin, or Class F coal fly ash (ASTM 2012; Chusilp et al. 2009). Physically, ash that passes a mesh ≤ 45 μm has a fine particle size that acts as a filler in concrete, thereby reducing its permeability (Chindaprasirt et al. 2007). Chemically, the appreciable concentrations of SiO_2, Al_2O_3, and Fe_2O_3 in ash can enhance the chemical binding in the concrete through a pozzolanic reaction. Specifically, amorphous SiO_2 in the ash is expected to react with $Ca(OH)_2$ that was generated from the cement hydration to form calcium silicate hydrate $[(CaO)_x \cdot (SiO_2)_y \cdot (H_2O)_z$; C−S−H] (Shi and Day 2000). Since C−S−H is the principal strength contributor in concrete, supplementary C−S−H formation by the pozzolanic reaction should further enhance concrete performance, giving it greater strength and more durability.

According to the previous work, ash from an open switchgrass combustion ($\approx$411°C for 5 min) contained 67.2% of SiO_2 (by weight), and 72.2% of its structure was amorphous (by unit) (Wang et al. 2014a). 10% of the cement was substituted with the ash ($\approx$ 65 μm of mean particle size) to test the strength of concrete test cylinders (50 mm diameter, 100 mm height). After 28 d curing in a moisture room at 23°C, concrete strength was 28.6 MPa, which was weaker than the concrete without ash replacement (32.5 MPa). The lower strength of concrete produced from a cement blend containing 10% ash was ascribed to its lower SiO_2 content (compared to silica fume, the conventional pozzolan containing 99% SiO_2) and insufficient amorphous phase in structure, since the SiO_2

[1]Ph.D. Candidate, Dept. of Natural Resource Sciences, McGill Univ., Ste-Anne-de-Belleuve, QC, Canada H9X 3V9.

[2]Associate Professor, Dept. of Civil Engineering and Applied Mechanics, McGill Univ., Montreal, QC, Canada H3A 0C3.

[3]Assistant Professor, Dept. of Mechanical and Materials Engineering, Queen's Univ., Kingston, ON, Canada K7L 3N6.

[4]Associate Professor, Dept. of Natural Resource Sciences, McGill Univ., Ste-Anne-de-Belleuve, QC, Canada H9X 3V9 (corresponding author). E-mail: joann.whalen@mcgill.ca

Note. This manuscript was submitted on August 26, 2014; approved on February 13, 2015; published online on April 6, 2015. Discussion period open until September 6, 2015; separate discussions must be submitted for individual papers. This paper is part of the ***Journal of Materials in Civil Engineering***, © ASCE, ISSN 0899-1561/04015040(10)/$25.00.

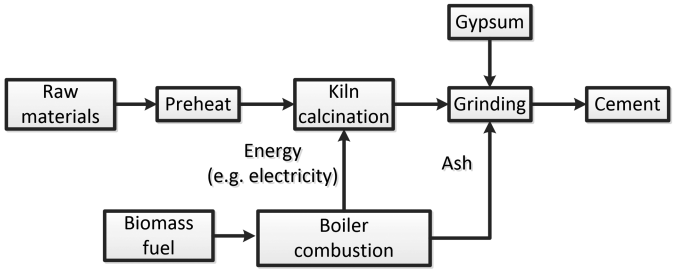

Fig. 1. The scenario of using an independent biomass combustion unit with ash recycling for sustainable cement production

concentration and amorphous structure determine the pozzolanic activity of ash (Jauberthie et al. 2000).

Adjusting the combustion conditions could feasibly enhance the pozzolanic properties of switchgrass ash and increase its recycling value for blending with cement. It is practical to control the biomass combustion at a certain temperature for a fixed retention time by changing the primary/secondary air-supply rate and feedstock conveying speed in a biomass boiler (e.g., moving-grate boiler) (Demirbas, 2005; Nussbaumer 2003). Ash structure should be amorphous predominately, which makes the SiO_2 chemically reactive during the pozzolanic reaction. The crystalline-amorphous microstructure of ash is determined by the original properties of switchgrass, and it can also be considerably affected by combustion conditions (Ataie and Riding 2013, 2014). For instance, Feng et al. (2004) found that an up to 800°C combustion produced a rice husk ash containing the highest amorphous SiO_2 of 95.7%. Yet, Xu et al. (2012) supported a 600°C combustion for the best amorphous ash. A low temperature (<500°C) cannot promote the transition from crystalline to amorphous phase, but amorphous structure was instead transformed back to crystalline phase by an overly high temperature (800°C). Hence, it should be possible to optimize the combustion process to generate ash with the desired level of pozzolanic activity. Cordeiro et al. (2009) found that the sugar cane bagasse ash from the 600°C combustion possessed the best pozzolanic activity due to its amorphous silica, low carbon content, and high specific surface area. Biricik et al. (1999) stated that wheat straw ash produced from combustion at 670°C for 5 h had a higher pozzolanic activity than that from 570°C combustion. Nair et al. (2008) asserted that carbon was not completely removed from rice husk ash when it was combusted at 300°C, whereas combustion at 500–700°C for 12 h generated ash with the best pozzolanic activity owing to its high amorphous silica content. Villar-Cociña et al. (2011) found that bamboo leaf ash (600°C combustion for 2 h) was totally amorphous, and recommended these parameters for combustion operations aiming to produce ash for blending with cement. These studies illustrate that careful control of combustion temperature and retention time can produce ash with advantageous pozzolanic activity.

Combustion temperature and time alter the physiochemical properties of ash, thus changing its pozzolanic performance (Zain et al. 2011). The amorphous change in ash structure can be estimated by a quantitative X-ray diffraction (XRD) analysis. However, this method still cannot indicate the pozzolanic activity unbiasedly, since pozzolanic reaction is determined by both chemical and physical properties of ash. Hence, a more precise analysis is further required, which is achieved by a numeric simulation model with kinetic analysis. Simulation is based on the experimental data of the conductivity or Ca^{2+} concentration [Ca^{2+}] in a $Ca(OH)_2$-ash suspension (Luxán et al. 1989). Villar-Cociña et al. (2003) explored the pozzolanic reaction of sugar cane straw ash and rice husk ash (combusted at 800°C or 1,000°C), generating experimental data for the simulation model by mixing 2.1 g of ash with 75 mL of saturated $Ca(OH)_2$ at 26 ± 1°C, and then recording conductivity change in the solution for a 624 h period. A similar method (2.1 g of ash +100 mL of $Ca(OH)_2$, at 26 ± 1°C in 50 h) was also used to evaluate the pozzolanic activity of bamboo leaf ash (combusted at 600°C for 2 h) (Villar-Cociña et al. 2011). Yet, as this method indirectly measured the reaction progress by conductivity, it could not discover the change of Ca^{2+} (as a principal reactant) during the pozzolanic reaction. These shortcomings were partially alleviated by the method of Donatello et al. (2010), who studied the change in [Ca^{2+}] in a $Ca(OH)_2$-pozzolan suspension [1 g of pozzolan +75 mL of $Ca(OH)_2$, at 40 ± 1°C]. However, since Ca^{2+} was titrated at room temperature (25–28°C) but $Ca(OH)_2$-pozzolan reaction occurred at 40 ± 1°C, this temperature difference would affect the accuracy of [Ca^{2+}] results because $Ca(OH)_2$ solubility was controlled by its negative heat of solution, leading to condensation of extra $Ca(OH)_2$ at 40°C [the temperature of $Ca(OH)_2$-ash reaction]. Consequently, this condensed $Ca(OH)_2$ would dissolve while the pozzolanic reaction occurred, thus affecting the accuracy of the result. Therefore, an unbiased method is needed to scrutinize the conductivity-[Ca^{2+}] correlation during the pozzolanic reaction, and also to improve the accuracy of the method by performing all steps at the same temperature.

In addition to the effect on ash properties, combustion temperature affects energy conversion from switchgrass. Typically, biomass combustion consists of a preparation step (moisture removal, ≤ 200°C), a fast combustion step (volatile pyrolysis, 200–500°C) and a slow combustion step (char calcination, ≥ 500°C) (Nussbaumer 2003). Mass loss from the fuel occurs mostly in the fast combustion step, with a longer char calcination period assuring that the carbon is totally transformed to CO_2 (complete combustion). Previous studies using thermogravimetric analysis-differential scanning calorimetry (TGA-DSC) (25–1,000°C) consistently proved that the highest energy conversion efficiency occurs when temperature is high enough to achieve complete combustion (Yuzbasi and Selçuk 2011; Haykırı-Açma 2003; Gil et al. 2010). As energy extraction is the principal objective of switchgrass combustion, the temperature effect on energy output and ash pozzolanic activity should be examined concurrently, especially when considering a LCF suitable for a cement plant.

This paper aimed to optimize switchgrass combustion to maximize the ash recycling value in cement and energy output concurrently. First, the combustion process was studied using temperatures of 350, 450, 550, and 650°C, and retention times of 1 and 4 h, and compared to ash from open combustion (as a control group). Combustion energy output at those temperatures was estimated by TGA-DSC, and ash pozzolanic activity was examined by measuring the strength of the concrete made from cement blended with 10% ash. Second, the crystal characteristics of switchgrass ash were evaluated with an unbiased method that relied on experimental data from $Ca(OH)_2$-ash suspensions to run a numeric simulation of the pozzolanic reaction. Kinetic parameters obtained from the simulation quantified the physiochemical change of ash and the conductivity-[Ca^{2+}] correlation during the pozzolanic reaction.

Material and Methods

Switchgrass Preparation and Characterization

Switchgrass was collected from a farm in Williamsburg, Ontario, Canada. Chemical composition of the switchgrass was analyzed by

the fusion inductively coupled plasma (ICP) method with a Varian Vista 735 ICP analyzer. Combustion profile of the switchgrass was characterized by the TGA-DSC with a NETZSCH TG 449 F3 Jupiter Analyzer. About 18 mg of fine switchgrass particle was placed in an Al_2O_3 crucible and heated to 900°C from 25°C in a 20% of O_2+ 80% of N_2 (by volume) atmosphere. Volume rate of the gas was 20 mL/min, and heating rate was 10°C/min. Consequently, mass loss (%) and enthalpy behavior (mW/mg) were transcribed throughout the entire combustion process. Based on the TGA-DSC results, energy output (kJ/g) from the combustion was estimated from Eq. (1)

$$\text{Energy output} = \int_0^{0.1\times T-2.78} 0.06 \times \left(\frac{dH}{dT} - \frac{dH'}{dT}\right) dt \quad (1)$$

where H (mW/mg) = heat flux of switchgrass sample; H' (mW/mg) = heat flux of background; t (min) and T (K) = time and temperature during the combustion.

Switchgrass Combustion

This work investigated the effect of combustion temperatures (350, 450, 550, and 650°C) and retention times (1 and 4 h) on the pozzolanic activity of ash (Table 1). Each test was replicated three times. Before the test, switchgrass was manually sheared to 0.5 cm long, and approximately 10 g of the switchgrass was placed in a crucible at a Nabertherm L 5/11 kiln with a gas ventilation system. Combustion was controlled at the target temperature for precisely 1 or 4 h. Then, ash was cooled to room temperature naturally before it was collected and weighted. Mass loss following combustion as a function of temperature and retention time was compared statistically using a two-factor analysis of variance (ANOVA) Fisher's LSD test (at 0.05 level). In addition, ash from open (uncontrolled) combustion was incorporated as a control group to compare the influence of a well-controlled combustion on ash properties. Open combustion was done in an 84 × 38 × 51-cm combustor, at ≈411°C for 5 min. All ash samples were ground with a laboratory steel ball mill for 30 s prior to further analysis.

Switchgrass Ash Characterization

As-received ash was characterized for its physiochemical, thermal, crystal, and microstructural properties. Ash from the open combustion (control group) was analyzed by a Brunauer Emmett Teller (BET) analyzer for its surface area. Its mineral oxide composition was determined by the X-ray fluorescence (XRF) method with a PW2400 wavelength dispersive XRF spectrometer. Thermal property of the ash (control group) (≈10.6 mg) was examined by the TGA-DSC (experimental method was the same as described for switchgrass thermal characterization). Consequently, some critical temperatures were estimated from the DSC curve, including glass transition point, crystallization point, and melting/vaporization zone. Ash from all combustion conditions was characterized for its crystalline structure by the XRD method with a Philips PW1710 powder X-ray diffractometer. Generator power of the X-ray was 40 kV/20 mA with Cu anode material, and scanning angle ranged from 5 to 100°2θ. Scanning step size was set at 0.04°2θ/s. Amorphous degree in structure was quantified by the Rietveld refinement using Chebyshev I algorithm (Winburn et al. 2000), which was simulated by a *PANalytical XRD software* suite. Ash microstructure was observed by the scanning electron microscope (SEM) with a FEI Inspect F-50 FE-SEM analyzer. Elemental mapping on the ash 550-4 was performed by an EDAX energy dispersive spectroscopy (EDS) with octane silicon drift detector (SDD).

Table 1. Experimental Treatments for Investigating the Impact of Switchgrass Combustion on Energy Conversion and Ash Recycling Value in Cement

Designation	Combustion type	Temperature (°C)	Retention time	Replication
Control	Open combustion	411	5 min	3
350-1	Controlled combustion	350	1 h	3
450-1	Controlled combustion	450	1 h	3
550-1	Controlled combustion	550	1 h	3
650-1	Controlled combustion	650	1 h	3
350-4	Controlled combustion	350	4 h	3
450-4	Controlled combustion	450	4 h	3
550-4	Controlled combustion	550	4 h	3
650-4	Controlled combustion	650	4 h	3

Concrete Compressive Strength Test

Compressive strength of concrete cylinders (50-mm diameter, 100-mm height) was tested to estimate the pozzolanic activity index of ash (Cheriaf et al. 1999; Shao et al. 2000). As described in Table 2, Blended cement was 90% portland cement (from Lafarge cement) and 10% ash. Concrete without ash replacement (100% portland cement) was considered as the reference standard. Chemical composition of the cement was quantified by the XRF, and its cementing property was approximated by Bogue's equation (Bogue 1929). Specific surface area and mean particulate size of the cement were analyzed with a Horiba laser scattering particle size analyzer. Water/(cement + ash) ratio was 0.55 by weight, and coarse/fine aggregate mass ratio was 1.86. After casting, concrete samples were cured in a moisture room at 23°C for 28 days. Compressive strength of concrete was then tested with a Sintech 30/G electromechanical compressor (three replicates). To statistically evaluate the impact of combustion temperature and retention time on the ash, compressive strength was interpreted by a two-way analysis of variance (ANOVA) with replication ($n = 3$) test (at 0.05 significance level). The pozzolanic activity index (PAI, %) of the ash was calculated from Eq. (2)

$$\text{PAI} = \frac{\text{Compressive strength}}{\text{Reference strength}} \times 100 \quad (2)$$

Moreover, for eliminating the disturbance of standard deviation on the PAI, a signal-to-noise ratio index (S/N) [Eq. (3)] was calculated to distinguish the best combustion condition for the greatest PAI by choosing the highest S/N value (Hew et al. 2010)

$$\frac{S}{N} = -10 \times \log_{10}\left[\frac{\sum_{j=1}^{3}\left(\frac{1}{P_{ij}}\right)^2}{3}\right] \quad (3)$$

where P_{ij} corresponded to the PAI of the jth replication in the ith ash sample group.

Table 2. Mixture Proportion of Portland Concrete and Switchgrass Ash for Compressive Strength Test

Mixture (kg/m^3)	Relative density (1)	100% cement (reference group)	90% cement + 10% ash
Portland cement	2.87	330	297
Fine aggregate	2.81	660	594
Course aggregate	2.61	1,226	1,103
10% ash	1.79	0	33
Water (w/b = 0.55)	—	182	182

Numeric Simulation of Pozzolanic Reaction

Pozzolanic Reaction Progress Measurement

For preparing a saturated $Ca(OH)_2$ solution, 2 g of $Ca(OH)_2$ powder (from Fisher Scientific) was dissolved in 1 L of water before filtration [to remove extra insoluble $Ca(OH)_2$]. For each ash sample, 2 g of the ash was added to a plastic bottle containing 75 ml of the saturated $Ca(OH)_2$ solution. The plastic bottle was sealed tightly to avoid carbonation and preserved at 25°C for 360 h. The solution was sampled every 24 h to measure the conductivity (mS/cm) and Ca^{2+} concentration ($[Ca^{2+}]$, mmol/L). Conductivity was tested with a temperature-compensated Fisher Scientific traceable conductivity meter. Ca^{2+} was titrated with 0.03 mol/L EDTA solution containing Patton and Reeders indicator. Additionally, calibration was done to obtain the conductivity-$[Ca^{2+}]$-pH correlation in a pure $Ca(OH)_2$ solution (Fig. S1). All measurements were replicated three times. Based on the experimental data, pozzolanic reaction progress index (ξ) was calculated by Eq. (4) or Eq. (5)

$$\xi - \text{conductivity} = \frac{y_0 - y_i}{y_0} \tag{4}$$

$$\xi - [Ca^{2+}] = \frac{z_0 - z_i}{z_0} \tag{5}$$

where ξ-conductivity or ξ-$[Ca^{2+}]$ = reaction progress calculated via the conductivity or $[Ca^{2+}]$ results; y_i and z_i symbolized the conductivity and $[Ca^{2+}]$ at $24 \times ih$; and y_0 and z_0 = initial value at 0 h.

Numeric Simulation

It is rational to simplify the pozzolanic reaction as a heterogeneous solid-solution process, which could be expressed by a pseudostable decreasing nucleus model (DNM) (Villar-Cociña et al. 2003). The pozzolanic reaction was assumed to be controlled simultaneously by ionic diffusion and chemical interaction. Based on these assumptions, numeric simulation was performed according to Eqs. (6) and (7) (Rosell-Lam et al. 2011)

$$\xi = 1 - \frac{0.23 \times e^{-3\times t/\tau} \times (-1 + e^{t/\tau}) \times \frac{1}{\tau}}{C_0 \times D_e \times r_s} + \frac{0.23 \times \frac{1}{\tau} \times e^{-t/\tau}}{C_0 \times K \times r_s^2} \tag{6}$$

$$K = \frac{K_B \times T}{h} \times e^{-\Delta G^{\#}/R\times T} \tag{7}$$

where ξ (1) = ζ-conductivity or ξ-$[Ca^{2+}]$; C_0 (mS/cm or mmol/L) = the initial value of conductivity or $[Ca^{2+}]$; t (h) = reaction time; D_e (mm^2/h) = diffusion coefficient; K (h^{-1}) symbolized a reaction rate constant; τ (h) = time interval until pozzolan nucleus decreased to 37% of initial value; r_s (mm) = radius of pseudostable solid in the solid-solution reaction ($r_s = 0.15$ mm); ΔG (kJ/mol) corresponded to the free energy of activation for the overall reaction; K_B and h = Boltzmann constant and the Planck constant, respectively; T (K) = absolute temperature; and R corresponded to the ideal gas constant.

Interpretation of Simulation Results

To statistically evaluate the impact of two ξ measurement method difference on the simulation results, a two-way ANOVA was conducted without replication test at 0.05 significance level. Ash sample variation and measurement difference (conductivity or $[Ca^{2+}]$) were considered as two independent variables in the test.

Table 3. Physiochemical Properties of Switchgrass and Its Ground Ash (As Control Group) from Open Combustion Test (≈ 411°C, 5 min) Followed by 30 s Steel Ball Mill Grinding

Mineral oxides (% by weight)	Switchgrass	Ground ash
SiO_2	2.23	67.2
Al_2O_3	0.250	0.680
Fe_2O_3	0.200	0.310
MnO	0.010	0.070
MgO	0.080	2.05
CaO	0.560	12.3
Na_2O	0.040	0.110
K_2O	0.140	1.24
TiO_2	0.010	0.060
P_2O_5	0.090	1.15
Loss on ignition (LOI)	96.4	14.8
Total	100	99.9
BET surface area (m^2/g)	—	41.3

Results and Discussion

Chemical and Thermal Properties of Switchgrass

Switchgrass used in this study contained, on average, 2.23% of SiO_2 and 0.56% of CaO (Table 3). Switchgrass had 1.04% of Si and the Si/Ca ratio was 2.60 (by weight), which guaranteed an adequate Si content for the pozzolanic reaction (Madani Hosseini et al. 2011). Switchgrass also had 96.4% loss on ignition (LOI), which was due to carbon and moisture removal as well as metal element evaporation at high temperature (e.g., Na_2O or K_2O, usually ≥ 800°C). As shown in the TGA-DSC profile (Fig. S2), the combustion profile of the switchgrass evidently consisted of three steps, including moisture removal (7.88% of mass loss, 25–254°C), fast volatile oxidization (55.1% of mass loss, 254–367°C) and slow char calcination (33.7% of mass loss, 367–900°C). During combustion, the maximal thermal decomposition rate (−1.68%/°C) occurred during the fast volatile oxidization stage (≈348°C), indicating that switchgrass combustion must reach at least 348°C to activate energy extraction. Switchgrass combustion was an exothermic process, which released 8.13 kJ/g of heat when temperature increased from 25 to 900°C (Fig. S3).

Combustion Test of Switchgrass

Increase in temperature (from 350 to 650°C) consistently raised the mass loss, an indicator of complete combustion, from 50.2 to 90.1% (1 h), or 54.0 to 91.4% (4 h) (Fig. S4). This was attributed to the slow char calcination in the high-temperature zone (367–900°C). Color of the ash changed from dark to white as the temperature increased (Fig. S5), which confirmed that more carbon in ash was removed by the char calcination. Moreover, longer retention (from 1 to 4 h) enhanced combustion. Prolonged retention boosted mass loss from 50.2 to 54.0% (350°C), and from 70.5 to 73.6% (450°C). Yet, there was no statistically significant difference between the two retention times when temperature was set at 550°C ($P = 0.150$) or 650°C ($P = 0.0.700$). This affirmed that higher temperatures were more effective than longer retention time to removing the carbon in ash. With a 4 h retention time, the TGA measurements were similar at each temperature tested ($P = 0.470$ at 350°C, $P = 0.750$ at 450°C, $P = 0.360$ at 550°C, and $P = 0.470$ at 650°C). This means that complete energy conversion of switchgrass can be achieved either by setting the temperature at 550–650°C for 1 h, or by lengthening the retention time to 4 h if temperature is set to 350–450°C.

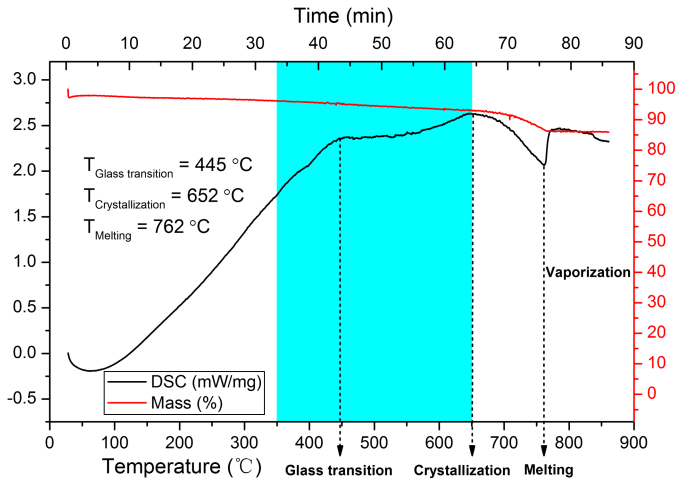

Fig. 2. Thermal characteristics of the switchgrass ash from open combustion (≈411℃, 5 min), used as a control group in this study

Characteristics of Switchgrass Ash

Pozzolanic properties of switchgrass ash were determined from its physiochemical, thermal, crystal, and microstructural characteristics. Ash from the open combustion (control group) had 41.3 m^2/g of BET surface area and contained 67.2% of SiO_2 by weight (Table 3). Its $SiO_2+Al_2O_3+Fe_2O_3$ was nearly 70% in total, which is categorized as Class C ash that could be recycled as a pozzolan in cement (ASTM 2012). However, its LOI was 14.8% by weight, which was attributed to the short retention time (5 min) and incomplete combustion. High volume of carbon would adversely affect the microstructure and concrete performance (Zain et al. 2011). When temperature increased from 25 to 900℃, mass loss of this ash was 14.1% (Fig. 2), similar to the LOI in Table 3. The entire process was exothermic (0.760 J/g of heat released), owing to the carbon removal from the ash. In the ash, glass transition and crystallization happened at 448 and 651℃, thereby the combustion between 448℃ and 651℃ would alter the proportion of amorphous forms substantially (Chindaprasirt et al. 2009; Cumpston et al. 1992). At higher temperatures (≥ 762℃), ash began to fuse and vaporize. Ash melting might cause a fouling and slagging problem in a combustor (e.g., moving-grate boiler), which lowers the energy efficiency (Teixeira et al. 2012).

Combustion temperature and retention time influenced the microstructure in ash. The XRD profile above a background curve demonstrated that all of the ashes were predominately amorphous, particularly in the zone of 20–40° 2θ (Fig. 3). Ash from the open combustion had the lowest amorphous silica content (78.2% by crystal unit). Still, a controlled combustion transformed more crystalline phase to amorphous form, and ash 550-4 had the greatest proportion of amorphous forms (85.8%). Longer retention time (4 h) increased the amorphous proportion from 83.6% (450-1) to 85.5% (450-4), and from 83.9% (550-1) to 85.8% (550-4). On the contrary, combustion temperature did not obviously influence the amorphous property of ash. Since a greater amorphous characteristic could advance the pozzolanic activity, prolonged combustion was beneficial to the ash recycling value for cement.

Microstructure in the ash mainly consisted of plates and debris, and it was affected significantly by combustion conditions. As shown in the SEM observation (Fig. 4), ash 350-1 had the least porous structure. Ash porosity increased greatly when combustion occurred at higher temperatures, either for 1 h or 4 h (samples 450-1, 550-4, and 650-4). High porosity might be the result of

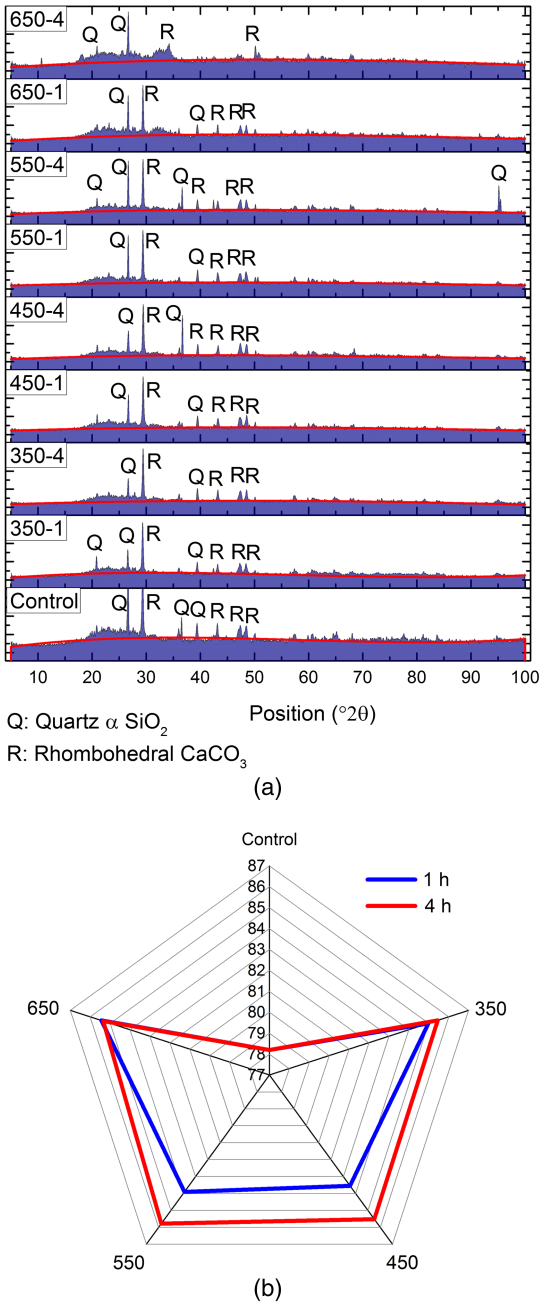

Fig. 3. (a) X-ray diffraction (XRD) profile (including the phase information) of the switchgrass ash from different combustion conditions. Control group was the ash from open combustion (≈411℃, 5 min); (b) comparison of amorphous structure proportion (%) of the ash samples

combustion that shattered the plates to debris (the ash 650-4). Compared to the ash from open combustion (67.2% of SiO_2), ash 550-4 possessed 85.2% of SiO_2 (Fig. S6), which confirmed that more carbon was removed by the higher temperature and longer retention time.

Compressive Strength of Concrete

Portland cement used in this study had a fine particle size of 22.0 μm. It was comprised of 65.6% of $(CaO)_3 \cdot (SiO_2)$ (abbreviated as C_3 S), 6.93% of $(CaO)_2 \cdot (SiO_2)$ (abbreviated as C_2 S), 12.7% of $(CaO)_3 \cdot (Al_2O_3)$ (abbreviated as C_3 A), and 8.49%

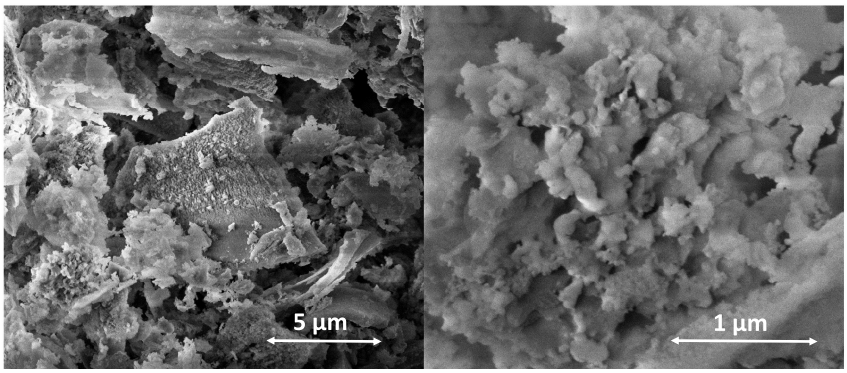

350 °C, 1 h
(a)

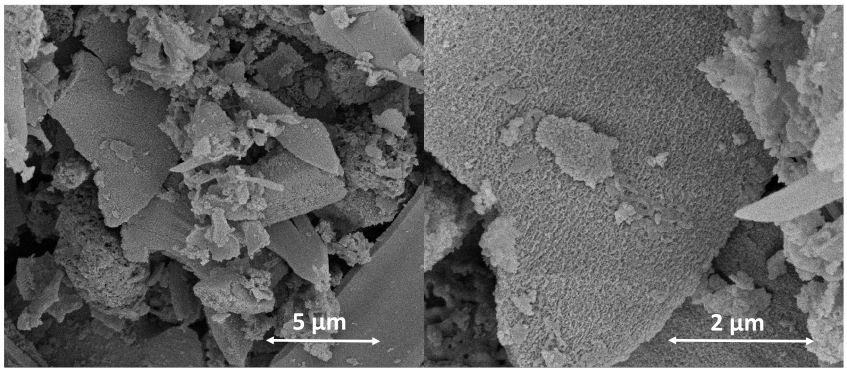

450 °C, 1 h
(b)

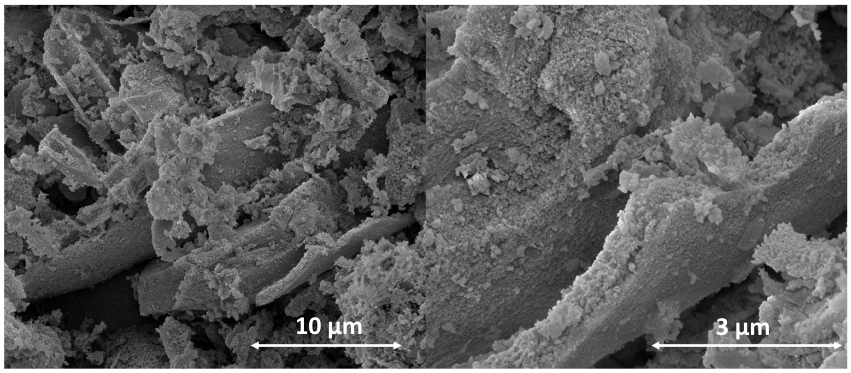

550 °C, 4 h
(c)

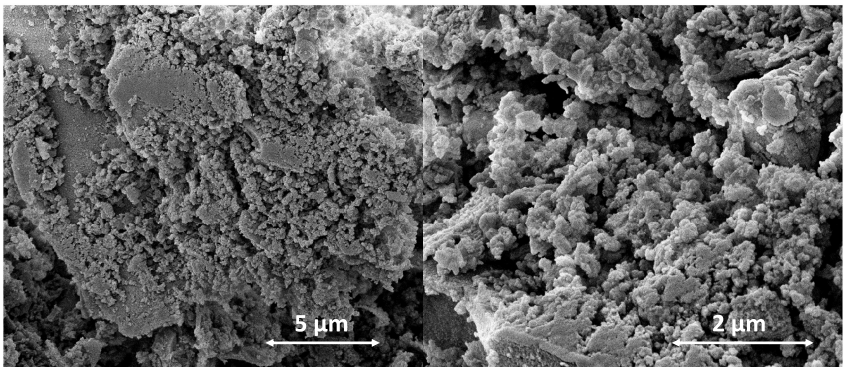

650 °C, 4 h
(d)

Fig. 4. Microstructural observation on selected ash samples by scanning electron microscopy (SEM): (a) the ash from the switchgrass combustion at 350°C for 1 h; (b) the ash from the switchgrass combustion at 450°C for 1 h; (c) the ash from the switchgrass combustion at 550°C for 4 h; (d) the ash from the switchgrass combustion at 650°C for 4 h

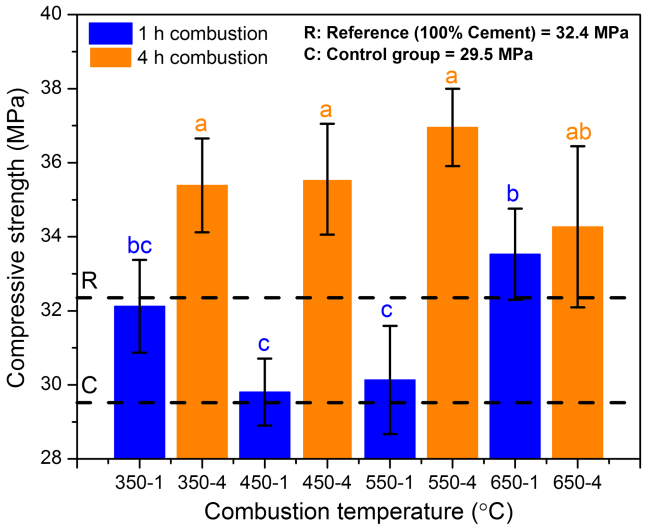

Fig. 5. Compressive strength of the concrete with 10% of the ash from different combustion conditions after 28 days curing in a moisture room at 23°C. Ash from open combustion was included as a control group, and is indicated as the dotted line C; concrete without ash replacement (100% portland cement) was considered as the reference group, with the dotted line R; values are the mean ($n = 3$) and standard deviation (error bars). Columns with different letters were significantly different at $P < 0.05$ level, assessed by a Fisher's LSD test

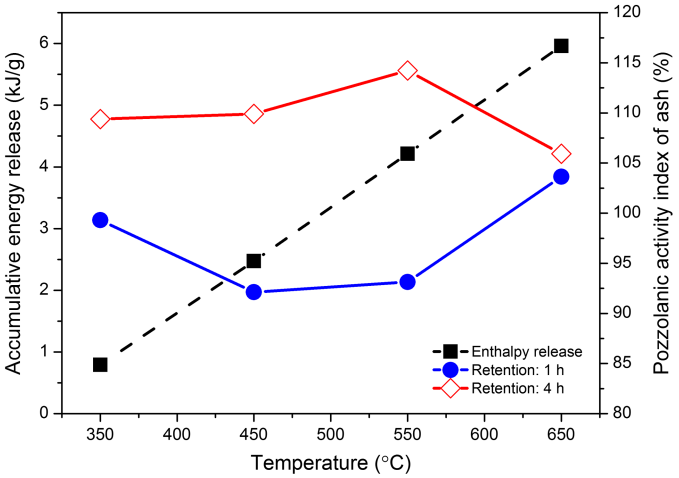

Fig. 6. Energy release of switchgrass combustion from 350 to 650°C, and pozzolanic activity index (%) of ash as affected by combustion conditions

of $(CaO)_4 \cdot (Al_2O_3) \cdot (Fe_2O_3)$ (abbreviated as C_4AF) (Table S1). After substituting 10% of the cement with ash, all ash samples from controlled combustion possessed greater compressive strength in concrete than the ash from open combustion (29.5 MPa after 28 d) (Fig. 5). This strength improvement was due to less carbon content and more amorphous forms in ash from controlled combustion, compared to the control group. However, strength of the sample 350-1 (32.1 MPa), 450-1 (29.8 MPa), and 550-1 (30.1 MPa) was slightly lower than the concrete with 100% portland cement (32.4 MPa, as a reference group). The explanation was that ash replacement diluted the initial cementitious proportion for hydration that creates C−S−H (as a primary strength contributor). On the contrary, ash from combustion with 4 h retention time consistently led to ≥ 32.4 MPa of strength. Since these ashes had the highest SiO_2 content (e.g., 85.2% in the ash 550-4) and also possessed a greater proportion of amorphous forms (85.4–85.8%), their pozzolanic reaction not only offset the dilution effect in cementitious composition from ash substitution but also contributed to supplementary C-S-H bond formation.

A two-way ANOVA with replication ($n = 3$) test revealed that retention time ($P = 2.17 \times 10^{-5}$) and temperature-retention interaction ($P = 0.0300$) had statistically influenced concrete strength (Table S2). However, combustion temperature did not significantly affect the strength ($P = 0.620$). Thus, adjusting retention time during a real combustion operation would be more efficient to optimize the ash recycling value than altering the temperature. Furthermore, as listed in Table S3, ash 550-4 had the highest signal-to-noise ratio at 41.1. This finding suggested that 550°C and 4 h were the optimal combustion conditions to generate ash with the highest pozzolanic activity.

Balance between Combustion Energy Output and Ash Pozzolanic Activity

When the temperature increased from 350 to 650°C, energy output from the switchgrass combustion monotonically increased from 0.790 to 5.96 kJ/g (Fig. 6). This relationship indicated that higher combustion temperature led to greater heat release. The ash from 4 h combustion had higher PAI (106–114%) than from the 1 h combustion (92.1–104%). Ash 550-4 exhibited the highest PAI, at 114%, which meant that ash 550-4 could enhance the concrete compressive strength by 14.2% compared to concrete with 100% portland cement. However, when combustion lasted for 4 h, an overly high temperature (650°C) instead degraded the PAI from 114 to 106%. The explanation was that a part of the amorphous structure was transformed to crystalline phase in this temperature zone. When considering combustion to optimize the ash recycling value and combustion energy output concurrently, this work suggested the temperature at 550°C and retention time for 4 h during switchgrass combustion.

Kinetic Simulation of Pozzolanic Reaction

Combustion Influence on Kinetic Parameters

Since saturated $Ca(OH)_2$ solution preparation, pozzolanic reaction, and measurement were conducted at the same temperature (25°C), this work could provide unbiased experimental data for the numerical simulation. Conductivity in a pure $Ca(OH)_2$ solution was strongly correlated to the $[Ca^{2+}]$ ($R^2 = 0.9857$, Fig. S1). Thus, there was an apparent similarity with two pozzolanic reactions in the $Ca(OH)_2$-ash suspension (measured via the conductivity or via the $[Ca^{2+}]$ in Fig. 7). However, there was appreciable divergence with different ash at the early and middle stages (0–250 h). In contrast, there was a minor discrepancy at the late stage (250–360 h), which was due to the complete consumption of SiO_2 from ash.

Kinetic parameters (diffusion coefficient D_e, chemical reaction rate constant K, constant of time τ, and free energy of activation ΔG) were evidently impacted by the ash with various pozzolanic activity (Table 4). Numeric simulation showed good correspondence with the experimental data, which was verified by a statistical parameter (R^2), as shown in Figs. S7 and S8. For all ash samples, D_e ($1.10 \times 10^{-3} - 6.30 \times 10^{-3}$ mm^2/h) was considerably lower than K ($0.900 \times 10^{-2} - 1.22 \times 10^{-2}$ h^{-1}). This relationship is interpreted to mean that diffusion speed of the reactants through the reaction product layer (around the reacting nucleus of the pozzolan particle) was slower than the chemical reaction rate at the nucleus

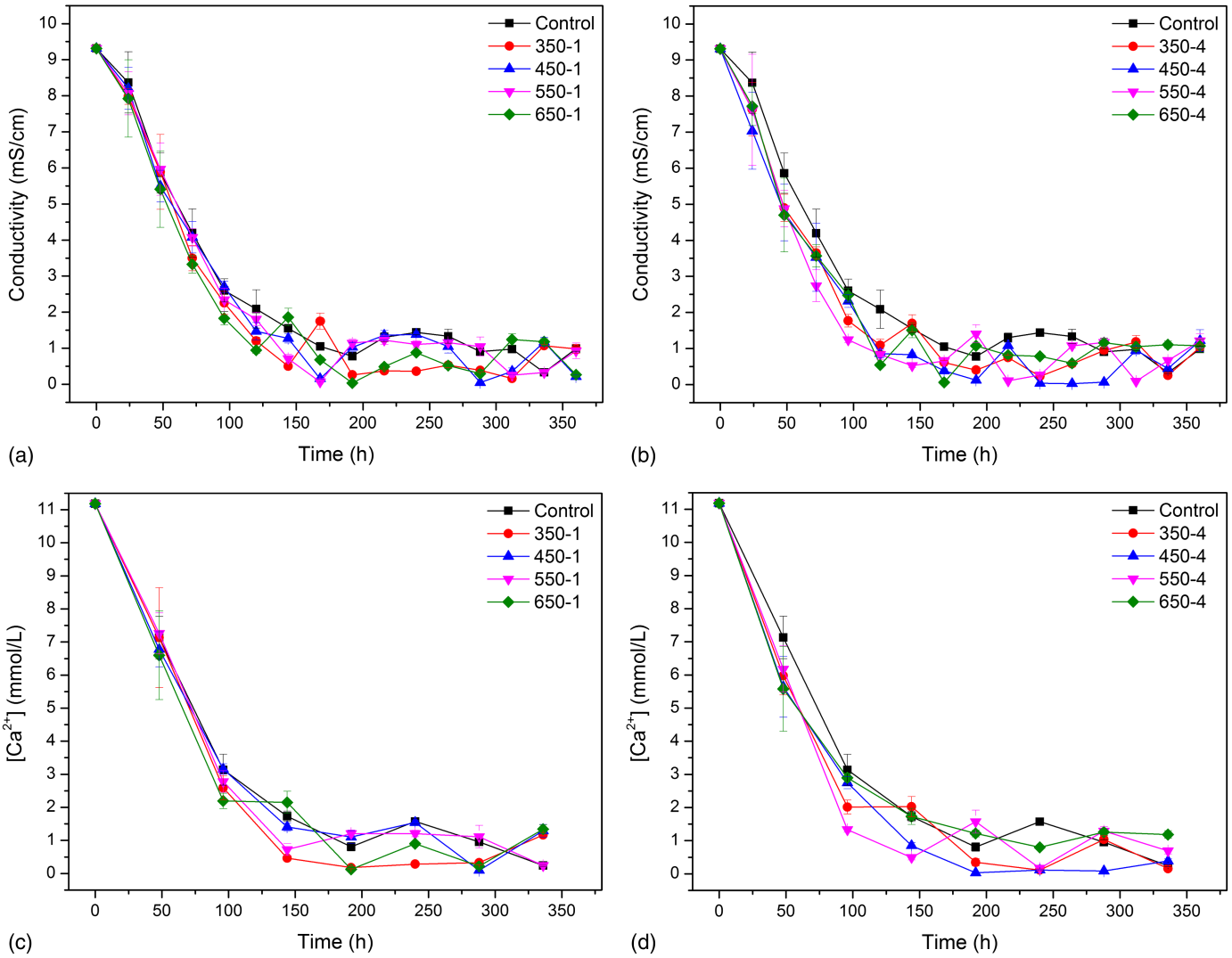

Fig. 7. Pozzolanic reaction progress of a $Ca(OH)_2$-ash suspension [2 g ash + 75 mL saturated $Ca(OH)_2$ solution], measured via the solution conductivity or Ca^{2+} concentration at each 24 h; (a) ash from switchgrass combustion at 350–650°C for 1 h, solution conductivity; (b) ash from switchgrass combustion at 350–650°C for 4 h, solution conductivity; (c) ash from switchgrass combustion at 350–650°C for 1 h, Ca^{2+} concentration; (d) ash from switchgrass combustion at 350–650°C for 4 h, Ca^{2+} concentration; control group was ash from open switchgrass combustion (≈411°C, 5 min)

surface. Accordingly, pozzolanic reaction rate in the $Ca(OH)_2$-ash suspension was principally limited by the ionic diffusion that might be affected by the porosity of pozzolanic reaction products.

Different combustion temperature and retention time changed the physical property (resulted in disparate D_e) and chemical reactivity (resulted in disparate K) of the entire solid-liquid system. Deviation with the chemical reactivity was attributed to various carbon removal degree (affected the SiO_2 purity) and different amorphous proportion in ash (affected the SiO_2 reactivity). As τ and ΔG were determined by the value of K, both τ and ΔG varied in proportion consequently. Compared to other ash samples, ash 550-4 had the least ΔG, at 62.1 kJ/mol or 62.3 kJ/mol. Because a lower ΔG was correlated with higher reactivity, pozzolanic reaction could process more easily and promptly.

Interpretation of Simulation Results

Analysis of the kinetic results (Table 4) demonstrated that the ash sample source had a significant influence on the K ($P = 0.0187$), but no impact on the D_e ($P = 0.393$), τ ($P = 0.124$), and ΔG ($P = 0.0602$) (Table S4). These differences indicated that varying the combustion temperature and retention time substantially changed the chemical interaction at the reaction product layer of ash-cement mixtures but did not affect the porosity. Thus, pozzolanic reaction rate in this study was controlled by ionic diffusion.

As conductivity was strongly correlated with the $[Ca^{2+}]$ in the pure $Ca(OH)_2$ solution (Adj. $R^2 = 0.9{,}857$, Fig. S1), kinetic results were hypothesized to be consistent if evaluated by conductivity measurement or the change in $[Ca^{2+}]$. However, ANOVA found that there was a significant difference for the K ($P = 0.00600$) and ΔG ($P = 0.0130$) but no difference for the D_e ($P = 0.510$) and τ ($P = 0.560$). This was because there was an extra pozzolanic contribution by other oxides in ash besides C–S–H. For instance, Al_2O_3 and Fe_2O_3 could interact with free $Ca(OH)_2$ and SiO_2 to form supplementary strength contributors in concrete microstructure, such as $(CaO)_x \cdot (Al_2O_3)_y \cdot (SiO_2)_z \cdot (H_2O)$w (abbreviated as C−A−S−H) or $(CaO)_x \cdot (Al_2O_3)_y \cdot (Fe_2O_3)_z \cdot (H_2O)_w$ (abbreviated as C−A−F−H). Since Al^{3+} and Fe^{3+} are conductive, this

Table 4. Kinetic Parameters from Numeric Simulation on $Ca(OH)_2$-Ash Suspension [2 g of Ash + 75 mL of Saturated $Ca(OH)_2$ Solution] Measured via Solution Conductivity or Ca^{2+} Concentration in Solution at Each 24 h

Sample	D_e (mm^2/h)	K (h^{-1})	τ (h)	ΔG (kJ/mol)
Parameters derived from solution conductivity				
Control	4.40×10^{-3}	1.35×10^{-2}	82.9	63.4
350-1	2.20×10^{-3}	1.84×10^{-2}	62.0	62.6
450-1	2.90×10^{-3}	1.59×10^{-2}	70.9	63.0
550-1	2.40×10^{-3}	1.66×10^{-2}	68.6	62.9
650-1	2.60×10^{-3}	1.88×10^{-2}	60.5	62.5
350-4	3.90×10^{-3}	1.78×10^{-2}	63.8	62.7
450-4	4.90×10^{-3}	1.86×10^{-2}	61.3	62.6
550-4	2.60×10^{-3}	2.21×10^{-2}	51.6	62.1
650-4	4.40×10^{-3}	1.74×10^{-2}	64.9	62.7
Parameters derived from Ca^{2+} concentration				
Control	3.30×10^{-3}	1.22×10^{-2}	78.0	63.6
350-1	1.10×10^{-3}	1.81×10^{-2}	52.6	62.6
450-1	6.00×10^{-3}	1.20×10^{-2}	79.1	63.7
550-1	1.50×10^{-3}	1.50×10^{-2}	63.3	63.1
650-1	3.00×10^{-3}	1.43×10^{-2}	66.3	63.2
350-4	6.30×10^{-3}	1.46×10^{-2}	65.0	63.2
450-4	3.80×10^{-3}	1.61×10^{-2}	59.0	62.9
550-4	1.20×10^{-3}	2.08×10^{-2}	45.6	62.3
650-4	1.20×10^{-3}	0.900×10^{-2}	105.3	64.4

Note: D_e (mm^2/h) = diffusion coefficient; K(h^{-1}) = chemical interaction rate constant; τ (h) = time interval until nucleus of pozzolan decreased to 37% of initial value; ΔG (kJ/mol) = free energy of activation for pozzolanic reaction.

explains why the numerical results for conductivity and the $[Ca^{2+}]$ in the $Ca(OH)_2$-ash suspension differed significantly.

Conclusions

Energy generation and ash recycling in cement could be optimized concurrently by adjusting the parameters of switchgrass combustion. When temperature went up from 350 to 650°C, energy output monotonically increased from 0.79 to 5.96 kJ/g. Controlled combustion transformed more crystalline to amorphous compounds in ash, although amorphous properties of ash were affected more by longer retention time than higher combustion temperature. Pozzolanic reaction involving ash from switchgrass combustion was controlled principally by ionic diffusion, a function of the ash elemental concentration of $SiO_2+Al_2O_3+Fe_2O_3$. Compared to ionic diffusion, chemical interaction in the reaction product layer of the $Ca(OH)_2$-ash mixture was more easily influenced by different combustion conditions. Consequently, this work suggested 550°C temperature and 4 h retention time for switchgrass combustion designed to generate energy and recycle ash in cement. Pozzolanic reaction in cement with 10% ash generated under these optimal conditions not only offset dilution effect in the cementitious composition due to ash substitution, but also improved the blended concrete strength by 14.2%. If the strategy of independent LCF combustion with ash recycling is extrapolated directly to an average-size cement production plant (3.06 GJ coal/1,000 kg cement product), CO_2 emissions could decrease by 1.77% within the entire life cycle when 5% of the coal burned is replaced by switchgrass energy with ash recycling.

Acknowledgments

This research was funded by Natural Science and Engineering Research Council (NSERC) of Canada and the McGill Collaborative Research Development Fund. The industrial support from Lafarge Cement North America was also appreciated.

Supplemental Data

Figs. S1–S8 and Tables S1–S4 are available online in the ASCE Library (www.ascelibrary.org).

References

ASTM. (2012). "Standard specification for coal fly ash and raw or calcined natural pozzolan for use in concrete." *C618–12a*, West Conshohocken, PA.

Ataie, F., and Riding, K. (2013). "Thermochemical pretreatments for agricultural residue ash production for concrete." *J. Mater. Civ. Eng.*, 10.1061/(ASCE)MT.1943-5533.0000721, 1703–1711.

Ataie, F., and Riding, K. (2014). "Use of bioethanol byproduct for supplementary cementitious material production." *Constr. Build. Mater.*, 51, 89–96.

Biricik, H., Aköz, Ö. F., Berktay, I. I., and Tulgar, A. N. (1999). "Study of pozzolanic properties of wheat straw ash." *Cem. Concr. Res.*, 29(5), 637–643.

Bogue, R. H. (1929). "Calculation of the compounds in portland cement." *Ind. Eng. Chem.*, 1(4), 192–197.

Cheriaf, M., Rocha, J. C., and Pera, J. (1999). "Pozzolanic properties of pulverized coal combustion bottom ash." *Cem. Concr. Res.*, 29(9), 1387–1391.

Chindaprasirt, P., Homwuttiwong, S., and Jaturapitakkul, C. (2007). "Strength and water permeability of concrete containing palm oil fuel ash and rice husk-bark ash." *Constr. Build. Mater.*, 21(7), 1492–1499.

Chindaprasirt, P., Jaturapitakkul, C., Chalee, W., and Rattanasak, U. (2009). "Comparative study on the characteristics of fly ash and bottom ash geopolymers." *Waste Manage.*, 29(2), 539–543.

Chusilp, N., Jaturapitakkul, C., and Kiattikomol, K. (2009). "Utilization of bagasse ash as a pozzolanic material in concrete." *Constr. Build. Mater.*, 23(11), 3352–3358.

Cordeiro, G. C., Toledo Filho, R. D., and Fairbairn, E. M. R. (2009). "Effect of calcination temperature on the pozzolanic activity of sugar cane bagasse ash." *Constr. Build. Mater.*, 23(10), 3301–3303.

Cumpston, B., Shadman, F., and Risbud, S. (1992). "Utilization of coal-ash minerals for technological ceramics." *J. Mater. Sci.*, 27(7), 1781–1784.

Demirbas, A. (2005). "Potential applications of renewable energy sources, biomass combustion problems in boiler power systems and combustion related environmental issues." *Prog. Energy Combust. Sci.*, 31(2), 171–192.

Donatello, S., Tyrer, M., and Cheeseman, C. (2010). "Comparison of test methods to assess pozzolanic activity." *Cem. Concr. Comp.*, 32(2), 121–127.

Feng, Q., Yamamichi, H., Shoya, M., and Sugita, S. (2004). "Study on the pozzolanic properties of rice husk ash by hydrochloric acid pretreatment." *Cem. Concr. Res.*, 34(3), 521–526.

Gil, M., Casal, D., Pevida, C., Pis, J., and Rubiera, F. (2010). "Thermal behaviour and kinetics of coal/biomass blends during co-combustion." *Bioresour. Technol.*, 101(14), 5601–5608.

Haykırı-Açma, H. (2003). "Combustion characteristics of different biomass materials." *Energy Convers. Manage.*, 44(1), 155–162.

Hew, K., Tamidi, A., Yusup, S., Lee, K., and Ahmad, M. (2010). "Catalytic cracking of bio-oil to organic liquid product (OLP)." *Bioresour. Technol.*, 101(22), 8855–8858.

Huntzinger, D. N., and Eatmon, T. D. (2009). "A life-cycle assessment of portland cement manufacturing: Comparing the traditional process with alternative technologies." *J. Cleaner Prod.*, 17(7), 668–675.

Jauberthie, R., Rendell, F., Tamba, S., and Cisse, I. (2000). "Origin of the pozzolanic effect of rice husks." *Constr. Build. Mater.*, 14(8), 419–423.

Jenkins, B., Baxter, L., Miles Jr, T., and Miles, T. (1998). "Combustion properties of biomass." *Fuel Process. Technol.*, 54(1), 17–46.

Luxán, M. P., Madruga, F., and Saavedra, J. (1989). "Rapid evaluation of pozzolanic activity of natural products by conductivity measurement." *Cem. Concr. Res.*, 19(1), 63–68.

Madani Hosseini, M., Shao, Y., and Whalen, J. K. (2011). "Biocement production from silicon-rich plant residues: Perspectives and future potential in Canada." *Biosyst. Eng.*, 110(4), 351–362.

Monti, A., Virgilio, N. D., and Venturi, G. (2008). "Mineral composition and ash content of six major energy crops." *Biomass Bioenergy*, 32(3), 216–223.

Nair, D. G., Fraaij, A., Klaassen, A. A., and Kentgens, A. P. (2008). "A structural investigation relating to the pozzolanic activity of rice husk ashes." *Cem. Concr. Res.*, 38(6), 861–869.

Nussbaumer, T. (2003). "Combustion and co-combustion of biomass: Fundamentals, technologies, and primary measures for emission reduction." *Energ. Fuel*, 17(6), 1510–1521.

PANalytical XRD software [Computer software]. Almelo, Netherlands, PANalytical.

Rosell-Lam, M., Villar-Cociña, E., and Frías, M. (2011). "Study on the pozzolanic properties of a natural Cuban zeolitic rock by conductometric method: Kinetic parameters." *Constr. Build. Mater.*, 25(2), 644–650.

Schneider, M., Romer, M., Tschudin, M., and Bolio, H. (2011). "Sustainable cement production present and future." *Cem. Concr. Res.*, 41(7), 642–650.

Shao, Y., Lefort, T., Moras, S., and Rodriguez, D. (2000). "Studies on concrete containing ground waste glass." *Cem. Concr. Res.*, 30(1), 91–100.

Shi, C., and Day, R. L. (2000). "Pozzolanic reaction in the presence of chemical activators: Part II—Reaction products and mechanism." *Cem. Concr. Res.*, 30(4), 607–613.

Teixeira, P., Lopes, H., Gulyurtlu, I., Lapa, N., and Abelha, P. (2012). "Evaluation of slagging and fouling tendency during biomass co-firing with coal in a fluidized bed." *Biomass Bioenergy*, 39, 192–203.

Villar-Cociña, E., Morales, E. V., Santos, S. F., Savastano Jr, H., and Frías, M. (2011). "Pozzolanic behavior of bamboo leaf ash: Characterization and determination of the kinetic parameters." *Cem. Concr. Comp.*, 33(1), 68–73.

Villar-Cociña, E., Valencia-Morales, E., González-Rodríguez, R., and Hernández-Ruíz, J. (2003). "Kinetics of the pozzolanic reaction between lime and sugar cane straw ash by electrical conductivity measurement: A kinetic-diffusive model." *Cem. Concr. Res.*, 33(4), 517–524.

Wang, Y., Shao, Y., Matovic, M. D., and Whalen, J. K. (2014a). "Recycling of switchgrass combustion ash in cement: Characteristics and pozzolanic activity with chemical accelerators." *Constr. Build. Mater.*, 73, 472–478.

Wang, Y., Winans, K., Shao, Y., and Whalen, J. K. (2014b). "Life cycle assessment: Applying biomass integrated gasification combined cycle in cement industry." *Proc., Environmental Science and Technology, the 7th Int. Conf. on Environmental Science and Technology*, Houston.

Winburn, R. S., Grier, D. G., McCarthy, G. J., and Peterson, R. B. (2000). "Rietveld quantitative X-ray diffraction analysis of NIST fly ash standard reference materials." *Powder Diffr.*, 15(3), 163–172.

Xu, W., Lo, T. Y., and Memon, S. A. (2012). "Microstructure and reactivity of rich husk ash." *Constr. Build. Mater.*, 29, 541–547.

Yin, C.-Y. (2011). "Prediction of higher heating values of biomass from proximate and ultimate analyses." *Fuel*, 90(3), 1128–1132.

Yuzbasi, N. S., and Selçuk, N. (2011). "Air and oxy-fuel combustion characteristics of biomass/lignite blends in TGA-FTIR." *Fuel Process. Technol.*, 92(5), 1101–1108.

Zain, M., Islam, M., Mahmud, F., and Jamil, M. (2011). "Production of rice husk ash for use in concrete as a supplementary cementitious material." *Constr. Build. Mater.*, 25(2), 798–805.